

1 Supporting Information

2 **A High-Thermal-Conductivity Composite Film for**
3 **Encapsulation and Passive Cooling of Solar Modules**

4 Yan Yang,^a Chao-Hua Xue,^{*a,b} Jun Cheng,^{*c} Li Wan,^b Hui-Di Wang,^b Wen-Jing Zhao,^b A-Jun Chang,^b

5 Qi Gao,^b Yan-Yan Yan,^b Xiao-Jing Guo^b

6 ^a College of Chemistry and Chemical Engineering, Shaanxi University of Science and Technology, Xi'an

7 710021, China.

8 ^b College of Bioresources Chemical and Materials Engineering, Shaanxi University of Science and

9 Technology, Xi'an 710021, China.

10 ^c Northwest Institute for Nonferrous Metal Research, Shaanxi Key Laboratory of Biomedical Metal

11 Materials, Xi'an 710016, China.

12 * Corresponding author.

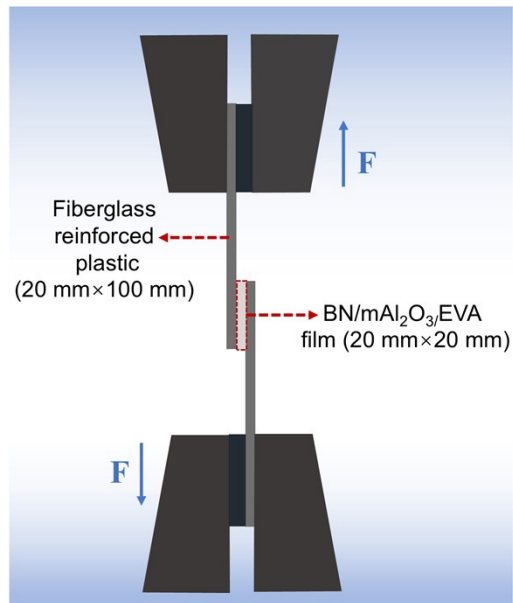
13 *E-mail address:* xuech@sust.edu.cn (C. H. Xue).

14 *E-mail address:* chengjun_851118@126.com

15

16

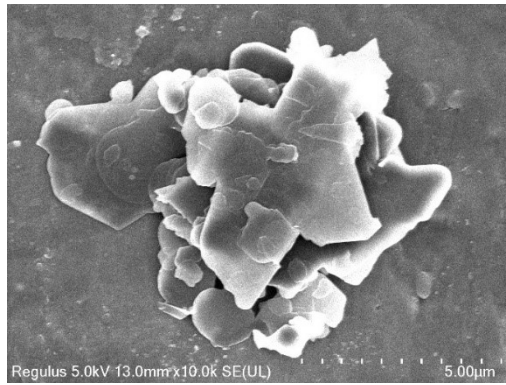
17



18

19 **Fig. S1** Schematic diagram of the test specimen for the shear strength of the composite film
20 and fiberglass-reinforced plastics.

21



22

23

Fig. S2 SEM image of h-BN.

24
25
26

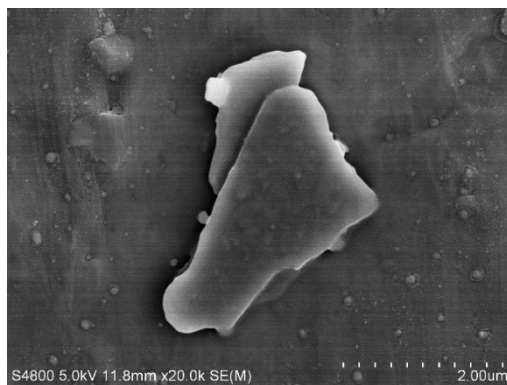
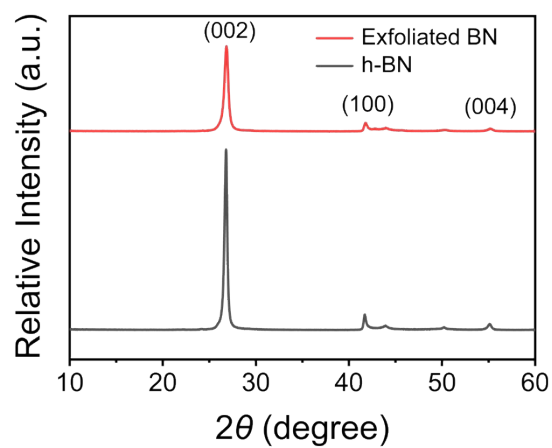


Fig. S3 SEM image of exfoliated BN.

27



28

29

30

Fig. S4 XRD patterns of h-BN and Exfoliated BN.

31
32
33

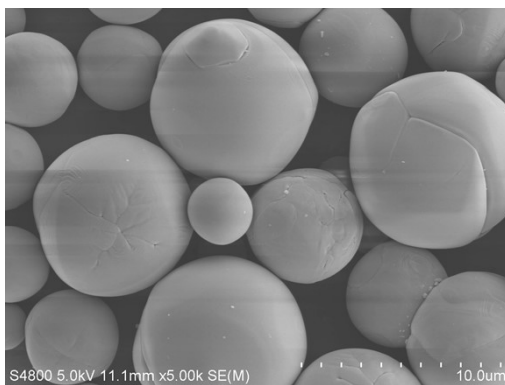


Fig. S5 SEM image of Al₂O₃.

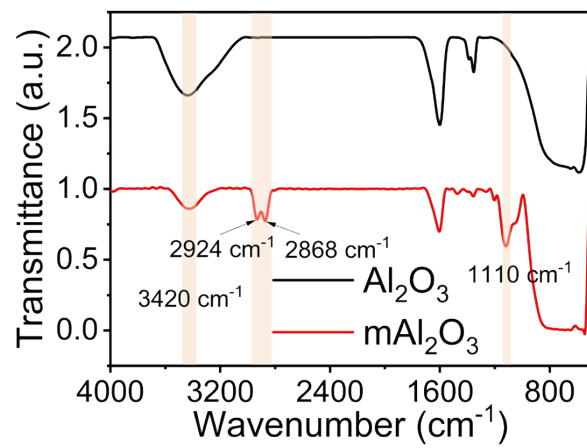
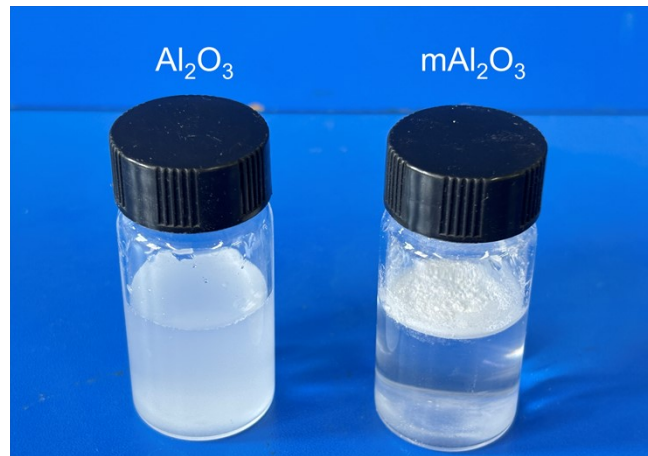


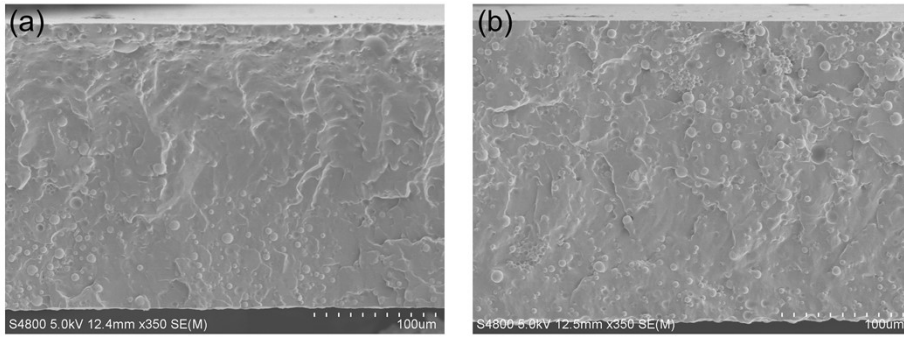
Fig. S6 FTIR spectra of Al₂O₃ and mAl₂O₃.

34
35
36



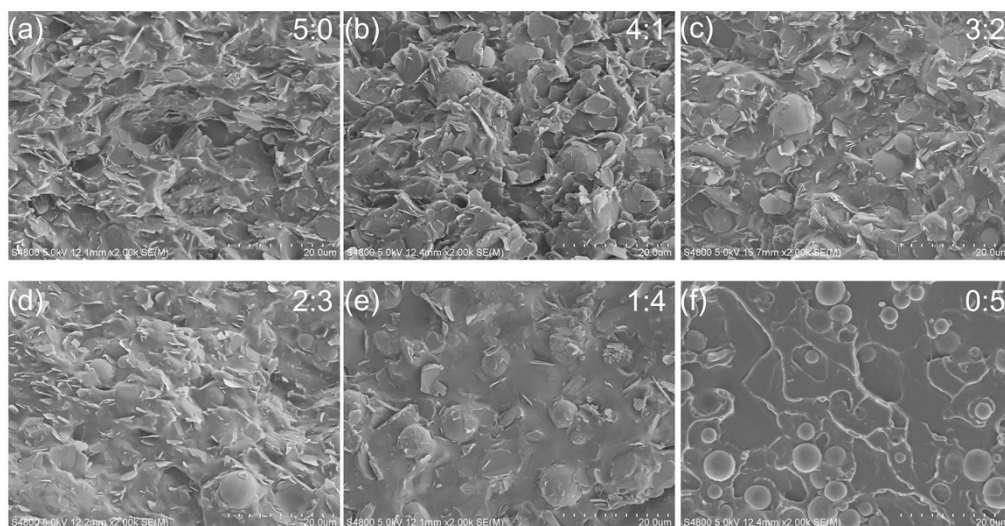
37

38 **Fig. S7** Optical photographs comparing the states of Al_2O_3 and mAl_2O_3 in water,
39 respectively. The mAl_2O_3 particles are floating above the water, indicating excellent
40 hydrophobicity.



41
42
43
44

Fig. S8 SEM images of (a) Al₂O₃/EVA and (b) mAl₂O₃/EVA.

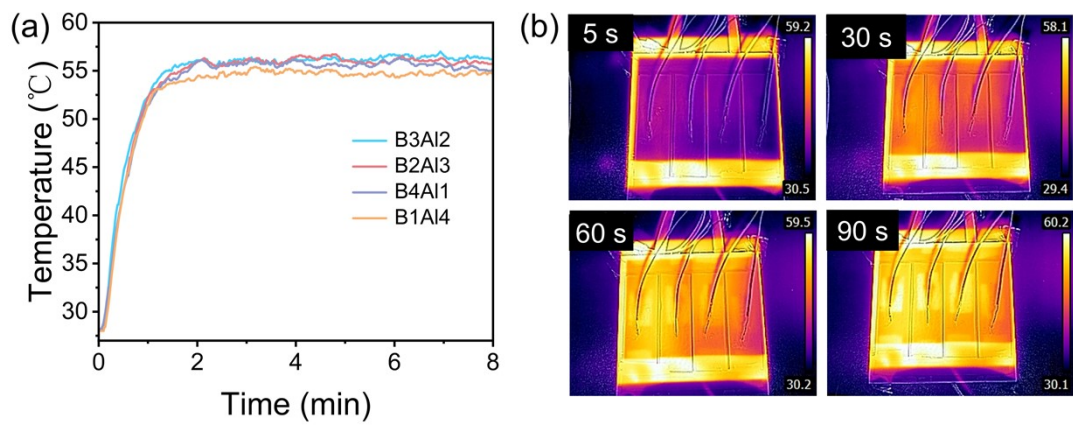


45

46 **Fig. S9** Cross-sectional SEM images of BN/mAl₂O₃/EVA film with different mass ratio: (a)
47 5 : 0, (b) 4 : 1 (c) 3 : 2, (d) 2 : 3, (e) 1 : 4, (f) 0 : 5.

48

49

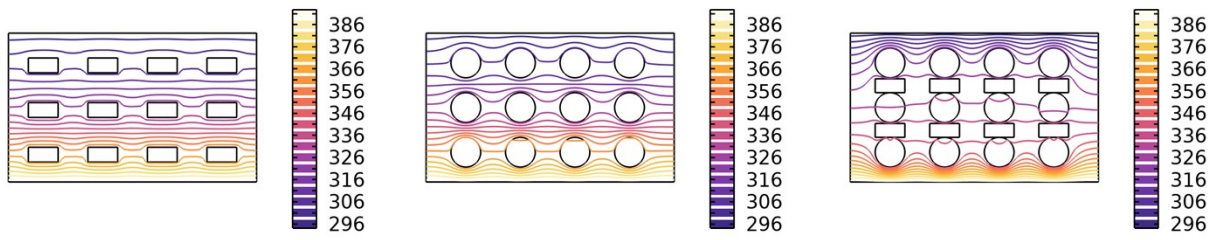


50

51 **Fig. S10** (a) Surface temperatures changes with heating time of the original B3A12, B2A13,
 52 B4A11 and B1A14 films on the hot stage; (b) Infrared thermal images of the corresponding
 53 films during the heating process from left to right, they are B3A12, B2A13, B4A11 and
 54 B1A14.

55

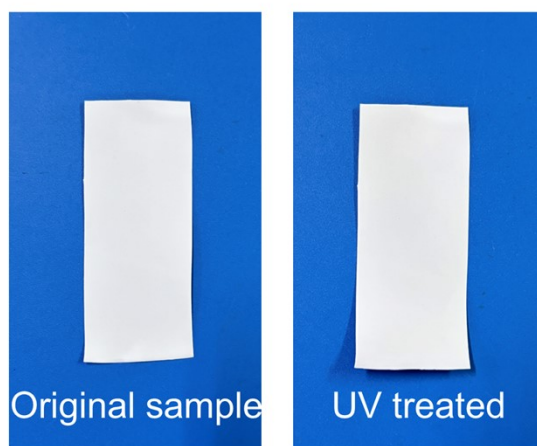
56



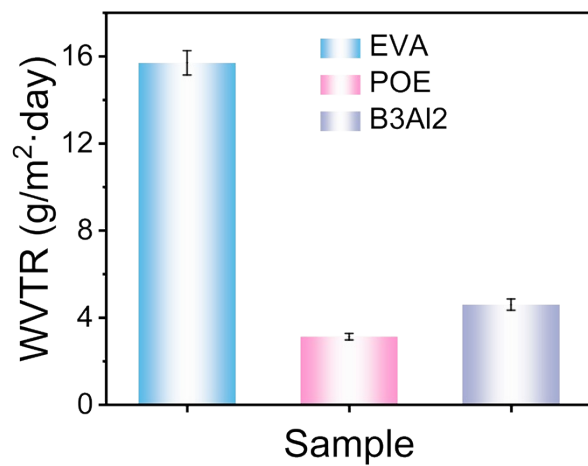
57

58 **Fig. S11** Linear isotherms of BN/EVA, mAl₂O₃/EVA, and BN/mAl₂O₃/EVA composite
59 films

60

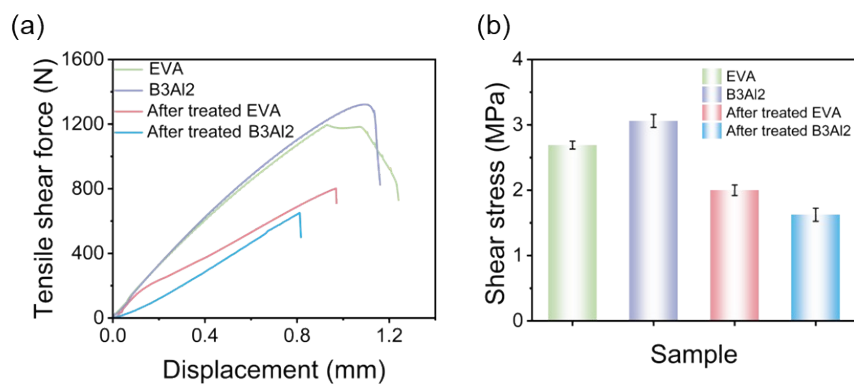


61
62 **Fig. S12** Photos of the B3A12 composite film before and after irradiation with ultraviolet
63 light for 720 hours.
64



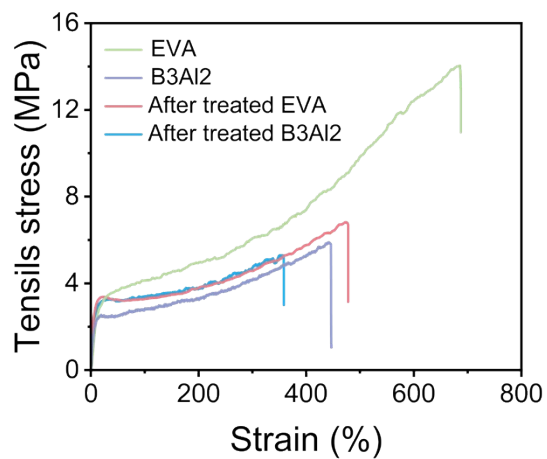
65

66 **Fig. S13** Water Vapor Transmission Rates of the EVA, POE and B3Al2 films



67

68 **Fig. S14** The load-displacement curves (a) and shear strength (b) of the EVA and B3Al2
 69 films before and after treatment of 720 hours of ultraviolet irradiation and 520 hours of
 70 treatment at 85°C and 85% humidity.



72

73 **Fig. S15** The tensile stress-strain curves of EVA, B3Al2 films before and after treatment of
74 720 hours of ultraviolet irradiation and 520 hours of treatment at 85°C and 85% humidity.

75 ¹

76

Table S1 Raw materials and their prices

Materials	Specification	Unit price (CNY/kg)
EVA particles	Photovoltaic grade, VA 28–33%	9
BN powder	Industrial grade, 99%, 1–3 μm	100
Al_2O_3 powder	Industrial grade, 99.5%, 1–5 μm , Silane modification	7.5

77

78 Table S2 Cost calculation of the pure EVA film and the BN/ Al_2O_3 /EVA film

Sample	EVA (kg)	BN (kg)	Al_2O_3 (kg)	EVA (CNY)	BN (CNY)	Al_2O_3 (CNY)	Total (CNY)
Pure EVA film	1	0	0	9	0	0	9
BN/ Al_2O_3 /EVA film	0.6	0.24	0.16	5.4	24	1.2	30.9

79 Note: Bulk procurement (≥ 10 tons, FOB China); total filler loading of the composite is 40 wt%; the mass
80 ratio of h-BN to mAl_2O_3 is 3 : 2; The cost comparison only accounts for the main materials, namely the
81 EVA matrix and inorganic fillers, and excludes processing fees, additives, taxes, profits, and other related
82 expenses.

83

84

Table S3 The cooling methods and performance comparison of the BN/mAl₂O₃/EVA film with reported photovoltaic packaging materials or backsheet materials.

Samples	Heat dissipation method	Thermal conductivity		Emissivity (%)	Reflectance (%)	Tensile strength (MPa)	Cooling effect (°C)	Ref
		In-plane (W/m·K)	Out-of-plane (W/m·K)					
BN@EVA	Heat conduction	0.65	/	~ 30	68.4	~ 3	1-1.5	2
polyamide/aluminum/PET/PA	Heat conduction	13.53	0.38	/	/	/	1-2	3
biochar-based PCM	Heat conduction	1.10	/	/	/	/	/	4
BN-EVA	Heat conduction	0.75	/	/	/	/	0.7	5
BN/LiBr/PVA	Radiative/Evaporative	4.3	/	94	92	0.221	3-9	6
EVA+ZnO	Heat conduction	0.8	/	/	/	/	1.7	7
TPX/SiO ₂	Heat radiation	/	/	85.6	/	/	1	8
BN/mAl ₂ O ₃ /EVA	Heat conduction/ Radiation/Light reflection	2.71	1.01	85.48	85.38	6	2.2	This work

References

1. U. Desai, B. Kumar Sharma, A. Singh and A. Singh, *Solar Energy*, 2022, **231**, 908-920.
2. X. Sun, J.-B. Wang, M.-Q. Liao, Q. You, Y. Zheng, Y. Liu, X.-H. Han, N. Qu and Z.-B. Zhao, *ACS Sustainable Chem Eng*, 2025, **13**, 2188-2196.
3. J. Oh, B. Rammohan, A. Pavgi, S. Tatapudi, G. Tamizhmani, G. Kelly and M. Bolen, 2018, **8**.
4. B. Hari, S. Suresh, R. K. Kottala and S. Praveenkumar, *J Energy Storage*, 2025, **122**.
5. J. Allan, H. Pinder and Z. Dehouche, *AIP Adv*, 2016, **6**, 035011.
6. X. Ran, C. Liu and B. Chen, *Journal of Materials Science & Technology*, 2026, **249**, 189-195.
7. H. I. Elqady, S. Ookawara, A. H. El-Shazly and M. F. Elkady, *Case Stud Therm Eng*, 2021, **26**.
8. X. Cui, X. Sun, L. Zhou and X. Wei, *Solar Energy*, 2023, **264**.